Misalignment Tolerant Diffractive Optical Networks

Deniz Mengu[1,2,3], Yifan Zhao[1,3], Nezih T. Yardimci[1,3], Yair Rivenson[1,2,3], Mona Jarrahi[1,3], Aydogan Ozcan[1,2,3*]
[1]*Electrical and Computer Engineering Department, University of California, Los Angeles, CA, 90095, USA*
[2]*Bioengineering Department, University of California, Los Angeles, CA, 90095, USA*
[3]*California NanoSystems Institute (CNSI), University of California, Los Angeles, CA, 90095, USA*
[*]*Corresponding author: ozcan@ucla.edu*

Abstract: Design of diffractive optical networks that are resilient against physical misalignments is reported. The success of this design framework is also experimentally demonstrated using 3D printed diffractive networks that operate at THz wavelengths.

1. Introduction

Diffractive Deep Neural Networks (D^2NN) [1] form an optical machine learning platform that is physically composed of a series of diffractive surfaces, trained using deep learning for a specific all-optical inference task. Previous work has demonstrated generalization capabilities of D^2NNs to unseen, new image data achieving e.g., >98% for classification of handwritten digits [2]. The number of trainable layers in a diffractive network has been reported to provide significant advantages in terms of all-optical information processing capacity, signal contrast and diffraction efficiency of D^2NNs [3,4]. However, the multi-layer architecture of these diffractive optical networks poses practical challenges regarding e.g., layer-to-layer misalignments and related fabrication tolerances.

Here, we present and experimentally demonstrate a new training scheme that enables diffractive networks to preserve their inference accuracy against undesired physical misalignments. This design strategy models the fabrication tolerances and physical misalignments as uniformly distributed random variables and introduces these variations in the training stage. Thereby, the deep learning-based evolution of the diffractive surfaces of a given D^2NN design adapts to accommodate potential misalignments in the physical implementation of a diffractive network, while still retaining its inference accuracy. We term this training strategy of incorporating potential misalignment errors as part of the optical forward model as "vaccination" and the resulting diffractive optical networks as vaccinated D^2NNs (v-D^2NNs) [5].

2. Results and Discussion

To demonstrate the efficacy of our training scheme, we focus on the 3D layer misalignments in object classification diffractive networks as shown in Fig. 1A. Based on this 5-layer diffractive design, a non-vaccinated D^2NN can achieve 97.77% blind inference accuracy for the classification of MNIST digits, with perfectly aligned layers. However, as soon as the diffractive layers experience unwanted shifts in axial (lateral) coordinates, the classification accuracy of the diffractive network decreases rapidly as shown by the blue curve in Fig. 1B (Fig. 1C). For instance, the non-vaccinated D^2NN can only attain 38.40% test accuracy when the diffractive layers are misaligned around the optical axis at random within the range $(-2.12\lambda, 2.12\lambda)$ along both x and y axes. Our vaccination strategy [5] mitigates this significant performance loss by introducing random 3D displacement vectors, $\boldsymbol{D}^{(l,i)} = (D_x^{(l,i)}, D_y^{(l,i)}, D_z^{(l,i)})$, as part of the forward training model, representing the unwanted errors in the location of the layer, l, at training iteration, i, along the x, y and z directions, respectively. All three components of $\boldsymbol{D}^{(l)}$ are modeled as uniformly distributed, independent random variables in the form, e.g. $D_x^{(l)} \sim U(-\Delta_x, \Delta_x)$. Accordingly, to vaccinate D^2NNs against lateral misalignments, we set $\Delta_x=\Delta_y=\Delta_{tr}$ so that at every iteration, i, all the diffractive layers are randomly misaligned around the optical axis building up resilience against lateral misalignments. For instance, under the same testing/misalignment conditions that the non-vaccinated D^2NN provides 38.40% blind test accuracy, the vaccinated D^2NN model with $\Delta_x=\Delta_y=\Delta_{tr}=2.12\lambda$ (purple curve in Fig. 1C) mostly recovers the performance loss and attains 94.44% blind testing accuracy. In addition, this new misalignment resilient D^2NN can provide a peak inference accuracy of 96.1% in the case of perfect alignment. Meaning that, the ~56% performance gain of the vaccinated D^2NN under physical misalignments comes at the expense of only 1.67% decrease in accuracy under ideal alignment conditions. Similar advantages can also be observed in the case of *axial* misalignment of the diffractive layers. For instance, under axial misalignments in the range $(-2.4\lambda, 2.4\lambda)$ along the optical axis, the D^2NN that is vaccinated against such misalignments using $\Delta_{z,tr}=2.4\lambda$ in the training (yellow curve in Fig. 1B), retains 97.39% inference accuracy while the non-vaccinated D^2NN can only offer 94.88% under the same conditions.

To experimentally demonstrate the success of our vaccination scheme, we compared the inference accuracies of non-vaccinated and vaccinated 5-layer D^2NNs that are composed of 3D printed diffractive layers modulating the incoming light at THz wavelengths (see Fig. 2A). For a fair comparison, 6 MNIST digits were selected among the test samples that are correctly classified by both networks with similar output signal contrast under perfect alignment conditions. The 3rd layers of both the non-vaccinated and vaccinated D^2NNs were placed at 13 different locations: 12 misaligned/shifted locations on *x*, *y*, and *z* (4 per axis) and the ideal position as shown Fig. 2A; for each case, the class scores synthesized by these diffractive networks in response to the 6 input digits for different positions of the 3rd diffractive layers were experimentally measured.[5] Figure 2B exemplifies the class scores for the input digits '0' and '5'. While the vaccinated D^2NN can make the correct class assignment at all misalignment positions of its 3rd diffractive layer for both input digits, the error-free diffractive network design fails to infer the correct data class 11 times (see Fig. 2B). Moreover, out of the 78 classification experiments per network (6 digits × 13 positions of 3rd diffractive layer), the non-vaccinated and vaccinated D^2NNs failed 23 and 2 times, respectively, illustrating the efficacy of the presented training strategy.

This vaccination scheme brings significant advantages in guiding the evolution of D^2NNs, preserving their inference capabilities despite potential fabrication artefacts and misalignments in their physical implementation.

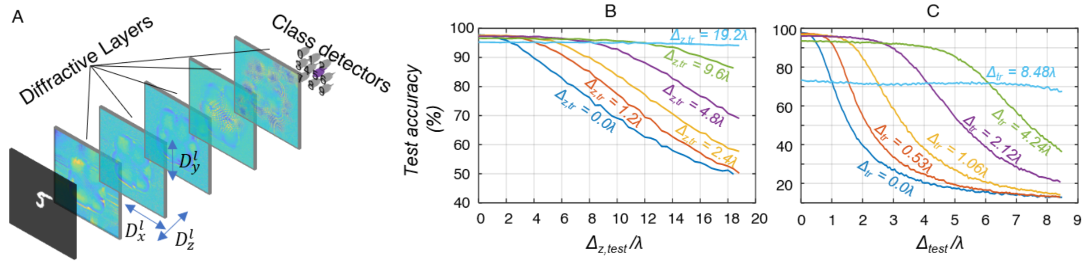

Fig. 1. Vaccination of diffractive optical networks classifying MNIST digits. (A) The layout of a 5-layer diffractive network. (B) Axial Misalignments: The blind inference accuracies achieved by error-free, $\Delta_{z,tr} = 0$ (blue), and vaccinated D^2NNs with $\Delta_{z,tr} = 1.2\lambda$ (red), 2.4λ (yellow), 4.8λ (purple), 9.6λ (green) and 19.2λ (light blue) under the presence of **axial layer-to-layer misalignments** created by $\Delta_{z,test}$ values between 0.0λ and 19.2λ. (C) Lateral misalignments: The blind inference accuracies achieved by error-free, $\Delta_{z,tr} = 0$ (blue), and vaccinated D^2NNs with $\Delta_x = \Delta_y = \Delta_{tr} = 0.53\lambda$ (red), 1.06λ (yellow), 2.12λ (purple), 4.24λ (green) and 8.48λ (light blue) **under the presence of lateral layer-to-layer misalignments** created by Δ_{test} values between 0.0λ and 8.48λ.

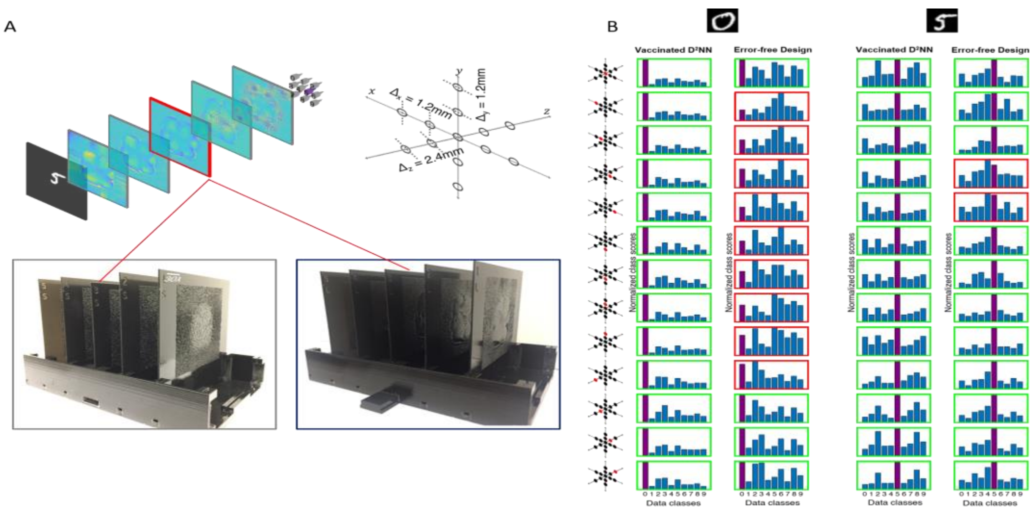

Fig. 2. Experimental results with 3D-printed diffractive networks. (A) The class inference of non-vaccinated (error-free) and vaccinated 5-layer diffractive networks were measured at 13 different locations of the 3rd diffractive layer including its ideal location. (B) Class scores obtained by the vaccinated and error-free D^2NNs at 13 different locations of their 3rd layer for two input samples, digits '0' and '5'. Green (red) frames around the measured class scores indicate correct (incorrect) inference results. The coordinate system on the left depicts the position of the 3rd layer for the corresponding class score measurements.

3. References

1. X. Lin, Y. Rivenson, N. T. Yardimci, M. Veli, Y. Luo, M. Jarrahi, and A. Ozcan, "All-optical machine learning using diffractive deep neural networks," Science **361**, 1004–1008 (2018).
2. J. Li, D. Mengu, Y. Luo, Y. Rivenson, and A. Ozcan, "Class-specific differential detection in diffractive optical neural networks improves inference accuracy," AP **1**, 046001 (2019).
3. D. Mengu, Y. Luo, Y. Rivenson, and A. Ozcan, "Analysis of Diffractive Optical Neural Networks and Their Integration With Electronic Neural Networks," IEEE J. Select. Topics Quantum Electron. **26**, 1–14 (2020).
4. O. Kulce, D. Mengu, Y. Rivenson, and A. Ozcan, "All-Optical Information Processing Capacity of Diffractive Surfaces," arXiv:2007.12813 [eees, cs, cs, physics] 28 (n.d.).
5. D. Mengu, Y. Zhao, N. T. Yardimci, Y. Rivenson, M. Jarrahi, and A. Ozcan, "Misalignment resilient diffractive optical networks," Nanophotonics **9**, 4207–4219 (2020).